Weyl fermions induced magnon electrodynamics in a Weyl semimetal

Jimmy A. Hutasoit, Jiadong Zang, Radu Roiban, and Chao-Xing Liu

Phys. Rev. B **90**, 134409 — Published 13 October 2014

DOI: 10.1103/PhysRevB.90.134409

Weyl fermions induced Magnon electrodynamics in Weyl semimetal

Jimmy A. Hutasoit,[1,*] Jiadong Zang,[2] Radu Roiban,[1] and Chao-Xing Liu[1]

[1] *Department of Physics, The Pennsylvania State University, University Park, Pennsylvania 16802*
[2] *Department of Physics, John Hopkins University, Baltimore, Maryland 21218*

(Dated: September 25, 2014)

Weyl fermions, which are fermions with definite chiralities, can give rise to anomalous breaking of the symmetry of the physical system which they are a part of. In their $(3+1)$-dimensional realizations in condensed matter systems, *i.e.*, the so-called Weyl semimetals, this anomaly gives rise to topological electromagnetic response of magnetic fluctuations, which takes the form of non-local interaction between magnetic fluctuations and electromagnetic fields. We study the physical consequences of this non-local interaction, including electric field assisted magnetization dynamics, an extra gapless magnon dispersion, and polariton behaviors that feature "sibling" bands in small magnetic fields.

In the 1980s, the study of anomalous behaviors of classically conserved currents in systems with Weyl fermions revealed a deep connection between this physical phenomena and the underlying topology of the systems. In particular, it was realized that these anomalies are deeply related to the skewness of the zero mode structure of the Dirac operators, which in turn, using index theorems, can then be related to characteristic classes, which are topological invariants[1–4]. Recently, with the advancement of realizations of topologically ordered condensed matter systems, the interest on the connection between topology and anomaly has been revived. Not only the study of anomalies might give rise to a way to classify topological phases in matters in the presence of interactions[5], but it can also lead to topological responses, which are physical manifestations of the underlying topological nature, of these topologically ordered systems[5–8].

In this letter, we study topological aspects of the Weyl semimetal, a topologically protected semimetal with Weyl fermions. Weyl semimetals can be regarded as a three-dimensional cousin of graphene, where pairs of bands cross at certain points in the momentum space, *i.e*, the Weyl points. For a short introduction to Weyl semimetals, see for example Ref. 9. Some material realizations of Weyl semimetals consist of topological insulator heterostructures that contain magnetic materials or magnetic dopants[10,11]. An advantage of this realization is that magnetic texture and fluctuations inherit some physical properties that reflect the underlying topological nature of this system. In particular, magnetic fluctuations are coupled to Weyl fermions as an axial vector field[12] and therefore, magnon excitations in this system possess topologically non-trivial electromagnetic responses from the axial anomaly.

Our main result takes the form of a non-local interaction between magnons and electromagnetic fields in Weyl semimetals, dictated by the effective action Eq. (4) below. The non-locality of the interaction arises from the fact that the mediators of this interaction are gapless excitations of Weyl fermions. The modifications of the Landau-Lifshitz (LL) equation and Maxwell equation due to this non-local interaction will give rise to two physical consequences, which reflect the underlying topological nature of Weyl semimetals. Firstly, in Weyl semimetals, electric fields can couple to the local magnetic moments through gapless Weyl fermions, leading to an additional magnon excitation. Compared to the conventional spin wave in ferromagnet, this new magnon branch is gapless and linear, inheriting the nature of Weyl fermions. Secondly, the non-local coupling between magnons and electromagnetic fields can induce a magnon-polariton excitations in Weyl semimetals, which exhibit a quite different spectrum from the usual polariton spectrum. In particular, in small values of magnetic fields, there exists a band with finite width that bifurcates into a pair of "sibling" bands with well-defined quasiparticles.

Let us start by considering a topological insulator doped with magnetic impurities and assume that magnetic moments are magnetized along the growth direction, which we will take to be the $\hat{x}_3$-direction. This system can be realized in for example, Cr doped Bi_2Te_3[13]. When magnetization is large enough, this model exhibits Weyl nodes, at which the effective excitations are two Weyl fermions with a relativistically-invariant dispersion relation. Thus, this system provides a natural description of Weyl semimetals using the 4-band model[12], the details of which are given in Appx. A. It turns out that in this system, magnetic fluctuations of magnetic moments are coupled chirally to Weyl fermions[12], and the effective action describing the interaction between Weyl fermions, electromagnetic fields and magnetic fluctuations is given by

$$S = i\int d^4x\, \bar{\psi}\gamma^\mu \left(\partial_\mu - ieA_\mu - ig\gamma_5 a_\mu\right)\psi, \qquad (1)$$

where two Weyl fermions have been written together as a single Dirac fermion ψ, A_μ is the electromagnetic gauge field and a_μ is an axial vector field whose space-like components $\mathbf{a}$ are identified as magnetic fluctuations[12]. Our convention for the γ matrices

$$\gamma^\mu = \begin{pmatrix} 0 & \sigma^\mu \\ \bar{\sigma}^\mu & 0 \end{pmatrix}; \quad \sigma^\mu = (\mathbb{1}_{2\times 2}, \sigma),\ \bar{\sigma}^\mu = (\mathbb{1}_{2\times 2}, -\sigma), \qquad (2)$$

and the metric follows closely Ref. 14, where the metric is mostly positive. In the following, we will consider only the case where the axial vector field strength $f_{\mu\nu} = \partial_\mu a_\nu - \partial_\nu a_\mu$ vanishes[15], which is the case when there is no magnetic domain wall in the system[12]. Even though we are not going to use this fact here, it is worth noting for $f_{\mu\nu} = 0$, the axial vector field can be written as $a_\mu = \partial_\mu \theta$, where θ has the physical meaning of axion fields[16].

To completely define this quantum field theory, it is necessary to specify a regularization scheme. This is particularly important here as the chiral nature of the interactions (1) implies that the theory exhibits an anomaly[17,18], which appears as a violation of current conservation in the three-point function $\Gamma^{\mu\nu\rho} = \langle j^\mu(p)\, j^\nu(q)\, j^{\rho 5}(-p-q)\rangle$, where $j^\mu = \bar\psi\gamma^\mu\psi$ and $j^{\mu 5} = \psi\gamma^\mu\gamma_5\psi$ are the $U(1)$ vector and axial current, respectively. The anomaly is a reflection of the impossibility of simultaneously preserving the vector and axial symmetries in the presence of any regulator. Since the vector symmetry characterizes the interaction of fermions and electromagnetic fields, the correct definition of the theory must include a regularization scheme that respects the vector symmetry, which is nothing but the gauge invariance of electromagnetism. An example of such scheme is the dimensional regularization scheme of 't Hooft and Veltman[19], and the calculation of $\Gamma^{\mu\nu\rho}$ using this scheme was done in Ref. 20. One can also calculate this three-point function using Cutkosky rules and the dispersion relation, as was done in Ref. 21. The result is

$$\Gamma^{\mu\nu\rho} = -\frac{ie^2 g}{2\pi^2}\,\varepsilon^{\alpha\mu\beta\nu}\,p_\alpha\,q_\beta\,\frac{g^{\rho\sigma}(p+q)_\sigma}{(p+q)^2}, \tag{3}$$

where $\varepsilon^{\alpha\beta\gamma\delta}$ is the totally antisymmetric Levi-Civita tensor.

It is easy to see that this three-point function satisfies the conservation of the vector current, $p_\mu\,\Gamma^{\mu\nu\rho} = 0 = q_\nu\,\Gamma^{\mu\nu\rho}$, but violates axial current conservation, $(-p-q)_\rho\,\Gamma^{\mu\nu\rho} = \frac{ie^2 g}{2\pi^2}\,\varepsilon^{\alpha\mu\beta\nu}\,p_\alpha\,q_\beta \neq 0$. We note that since anomalies are infrared phenomena (see for example, Ref. 22 and references within), we can expect the topological electromagnetic response of magnons to be insensitive to the details of the model away from the Weyl points as long as the electromagnetic gauge invariance is not broken. In a classic (particle physics) example, a similar anomaly is responsible for the decay of a neutral pion into two photons independently of the high energy completion of the theory of strong interactions that does not break the electromagnetic gauge invariance. For example, the pion decay is independent of the QCD quark masses[17,18]. Nevertheless, it will be interesting to study the non-topological electromagnetic response of magnons from the high energy sector of Weyl semimetals and such study will be taken up elsewhere. For the rest of this letter, we will focus on studying the physical consequences of the anomalous term Eq. (3).

To that end, we construct the effective action of the topological electromagnetic response of magnons as follows

$$\begin{aligned} S_{\rm top} &= \int \frac{d^4p}{(2\pi)^4}\frac{d^4q}{(2\pi)^4}\,\Gamma^{\mu\nu\rho}A_\mu(p)A_\nu(q)a_\rho(-p-q) \quad (4)\\ &= -\frac{e^2 g}{8\pi^2}\int d^4x\,d^4y\,\varepsilon^{\alpha\beta\gamma\delta}\,F_{\alpha\beta}(x)\,F_{\gamma\delta}(x)\,\frac{\partial G(x-y)}{\partial y^\mu}\,a^\mu(y), \end{aligned}$$

where $F_{\mu\nu} = \partial_\mu A_\nu - \partial_\nu A_\mu$ is the (vector) field strength, $G(x-y)$ is the Green function of the d'Alembertian $\Box = \partial_\mu\partial^\mu$ and it obeys $\Box_x\, G(x-y) = \delta^4(x-y)$.

We note that in the limit of a constant axial vector a^μ we recover the result of Refs.[23,24]. For details, see Appx. B. Furthermore, using the definition $j^\alpha = \delta S/\delta A_\alpha$, we can obtain the anomalous Hall response

$$j^\alpha(x) = -\frac{e^2 g}{2\pi^2}\,\varepsilon^{\alpha\beta\gamma\delta}\,F_{\gamma\delta}(x)\,\partial_\beta\int d^4y\,\frac{\partial G(x-y)}{\partial y^\mu}\,a^\mu(y), \tag{5}$$

which, in the limit of a constant axial vector a^μ, reduces to the known result $j^\alpha = -\frac{e^2 g}{2\pi^2}\,\varepsilon^{\alpha\beta\gamma\delta}a_\beta\,F_{\gamma\delta}$ of Ref. 25.

As another non-trivial check, we can also compare the effective action Eq. (4) with the result from 4-band model of Ref. 12 at uniform magnetic field $\mathbf{B} = B\,\hat x_3$, akin to the calculation done in Ref. 26. In this case, we have Landau levels and we can ask how the system responses to an applied electric field $\mathbf{E} = E\,\hat x_3$ and a perturbation due to magnetization. The result agrees with Eq. (4) and for details, see Appx. A.

We are now ready to study the modifications of LL and Maxwell equations caused by the topological response of Eq. (4). Assume an easy axis anisotropy is present such that the magnetic moments are uniformly polarized along the $\hat x_3$ direction in equilibrium. The magnon excitations are investigated by considering the magnetization dynamics of the following Hamiltonian:

$$H_{\rm magnet} = \frac{1}{2}\left(J\,(\nabla\mathbf{M})^2 + m^2\,|\mathbf{M}_\parallel|^2\right) - \mathbf{B}\cdot\mathbf{M}, \tag{6}$$

where $\mathbf{M}$ is the magnetization, $\parallel$ denotes the in-plane direction, $\mathbf{B}$ is the magnetic field, and m^2 is the easy axis anisotropy. Let $\mathbf{M} = M\,\hat x_3 + \mathbf{a}$, with $M \gg a_i$. Substituting Eqs. (4) and (6) into the LL equation

$$\frac{d\hat{\mathbf{M}}}{dt} = \gamma\hat{\mathbf{M}}\times\frac{\partial(H_{\rm magnet}+H_{\rm top})}{\partial\hat{\mathbf{M}}}, \tag{7}$$

we then have

$$\begin{aligned} \frac{\partial_t a_1}{\gamma M} &= -\frac{e^2 g}{8\pi^2}\int d^4y\,\varepsilon^{\alpha\beta\gamma\delta}F_{\alpha\beta}(y)F_{\gamma\delta}(y)\,\partial_2 G(x-y)\\ &\quad + B_2 + \left(J\,\nabla^2 - m^2 - B_3/M\right)a_2, \quad (8)\\ \frac{\partial_t a_2}{\gamma M} &= \frac{e^2 g}{8\pi^2}\int d^4y\,\varepsilon^{\alpha\beta\gamma\delta}F_{\alpha\beta}(y)F_{\gamma\delta}(y)\,\partial_1 G(x-y)\\ &\quad - B_1 - \left(J\,\nabla^2 - m^2 - B_3/M\right)a_1, \quad (9) \end{aligned}$$

where γ is the product of the gyromagnetic ratio, Bohr magneton and permeability of vacuum. It is interesting to note that a spatial-dependent term contributed from

the Weyl fermion enters the magnetization dynamics. It plays the same role as the in-plane magnetic field B_1 or B_2. The magnetic moments experience this spatially modulated effective field such that the magnon dispersion can be significantly changed. As the electromagnetic field strength $F_{\alpha\beta}$ contains electric fields as its component, it is quite interesting to see that the electric field can dramatically modify magnetization dynamics. To illustrate this more clearly, let us consider Weyl semimetals in a magnetic field along the $\hat{x}_3$ direction $\mathbf{B} = B_3\hat{x}_3$. For an oscillating electric field $\mathbf{E} = E_3 \exp\left(i\omega t - i\mathbf{q}_\parallel \cdot \mathbf{x}_\parallel\right) \hat{x}_3$, we obtain

$$\mathbf{a}_\parallel(\omega, \mathbf{q}_\parallel) = -\frac{ie^2 g}{\pi^2} \frac{(J\,q^2 + m^2 + B_3/M)\,\mathbf{q}_\parallel}{\omega^2/(\gamma^2 M^2) - (J\,q^2 + m^2 + B_3/M)^2} \frac{E_3\,B_3}{\omega^2 - v_F^2\,q^2}, \tag{10}$$

where $q = |\mathbf{q}_\parallel|$. Here, we have inserted back the Fermi velocity of the Weyl fermions in order to differentiate it with the speed of light in the medium, which we are taking to be unity.

Two poles of $\mathbf{a}_\parallel(\omega, \mathbf{q}_\parallel)$ suggest the existence of two magnon branches in this system. In addition to the usual spin wave $\omega = \gamma\,M\,(J\,q^2 + m^2 + B_3/M)$, a magnon with $\omega = v_F\,|q|$ is present. This novel dispersion is determined solely by a property of the Weyl fermions, namely their Fermi velocity. More importantly, this new branch is gapless, leading to a long-range correlation of spin excitations. Physically, this magnon excitation can be understood as a direct result of the coupling between two magnetic moments mediated by Weyl fermions. The gapless nature of Weyl fermions leads to long-range correlation of this magnon excitation. Therefore, this new magnon dispersion is a distinct feature of Weyl semimetals. One can then employ neutron scattering experiments to test our prediction.

Let us now look at the Maxwell equation in the presence of topological response of Eq. (4). It is given by

$$-\partial_\alpha F^{\alpha\beta} - \frac{e^2 g}{2\pi^2}\,\varepsilon^{\alpha\beta\gamma\delta} F_{\gamma\delta} \int d^4y\,\frac{\partial G(x-y)}{\partial x^\alpha}\,\frac{\partial a^\mu(y)}{\partial y^\mu} = 0. \tag{11}$$

By using the identity $\varepsilon_{\mu\nu\rho\sigma}\partial^\rho F^{\mu\nu} = 0$ and keeping only the linear term in $\mathbf{E}$, we get

$$-\partial_t^2 \mathbf{E} + \nabla^2 \mathbf{E} - \frac{e^2 g}{\pi^2}\,\mathbf{B} \int d^4y\,\partial_t^2 G(x-y)\;(\nabla\cdot\mathbf{a})\,(y) + \frac{e^2 g}{\pi^2}\,\nabla\,(\mathbf{B}\cdot\nabla) \int d^4y\,G(x-y)\;(\nabla\cdot\mathbf{a})\,(y) = 0. \tag{12}$$

For concreteness, let us again consider applying a uniform magnetic field B_3 along the $\hat{x}_3$ direction. If we shine a light with the electric field $\mathbf{E} = E_3 \exp\left(i\omega t - i\mathbf{q}_\parallel \cdot \mathbf{x}_\parallel\right) \hat{x}_3$, we have

$$\left[\omega^2 - q^2 - \left(\frac{e^2 g\,B_3}{\pi^2}\right)^2 \frac{q^2\,\omega^2}{(\omega^2 - v_F^2\,q^2)^2} \frac{J\,q^2 + m^2 + B_3/M}{\omega^2/(\gamma^2 M^2) - (J\,q^2 + m^2 + B_3/M)^2}\right] E_3(\omega, \mathbf{q}) = 0. \tag{13}$$

The solutions of the equation above correspond to the poles of the polariton modes, which can then be detected using various spectroscopy techniques, such as angle-resolved electron energy-loss spectroscopy. In a typical magnetic material, in the long wavelength regime, the effective magnon velocity $2\gamma M J q$ is significantly smaller than the Fermi velocity of the Weyl fermions. Thus, the dispersion of the magnon can be neglected. The typical behavior of the real part of the poles are plotted in Fig. 1. See also Appx. C.

One can find four bands in total in Fig. 1. These solutions represent the hybridization between electric fields and magnetic moments due to the non-local coupling induced by Weyl fermions. At a non-vanishing magnetic field, the top and bottom bands are non-degenerate. Furthermore, the imaginary parts of their respective poles vanish and therefore, their spectral density is given by a Dirac δ-function. The intermediate band, however, acquires a non-vanishing imaginary part of its pole and therefore, feature broadened spectral density. This broadening is due to its ability to emit Weyl fermions, which results in it acquiring complex self-energy. This is not unlike the physics of plasmon, see for example Ref. 27. At a low magnetic field, this band bifurcate into a pair of "sibling" bands, whose spectral densities are given by Dirac δ-functions, where the threshold for emitting Weyl fermions is beyond the energetics. As the magnetic field increases, this bifurcation disappears. The value of magnetic field at which this happens scales as g^{-2} and for $g \sim 0.1$, this value is of order 10 T.

At a small q, the top and bottom bands scale as $\omega \sim q^0$ and q^2, respectively, while the intermediate band scales like $\omega \sim q^{1/2}$. We note that for the intermediate band, there is a regime where the velocity of the latter exceeds the speed of light in the Weyl semimetal. This "tachyonic" regime needs to be excised, similar to the case of surface optical phonon for a polar crystal such as NaCl[28].

The polariton spectrum also features an energy range at which there exists no polariton modes. This "forbidden" band is particularly manifest at larger values of magnetic field. Therefore, the incident light will be totally reflected if its frequency lies within the forbidden band. Such forbidden band is predicted to be a generic feature of topological magnetic insulator[29], however, sibling bands are particular to the Weyl semimetal.

In order to probe the polariton, it is crucial that the energy dumped into the system is spent to excite the polariton and not the Weyl fermions. In other words, the observability of the polariton spectrum depends heavily

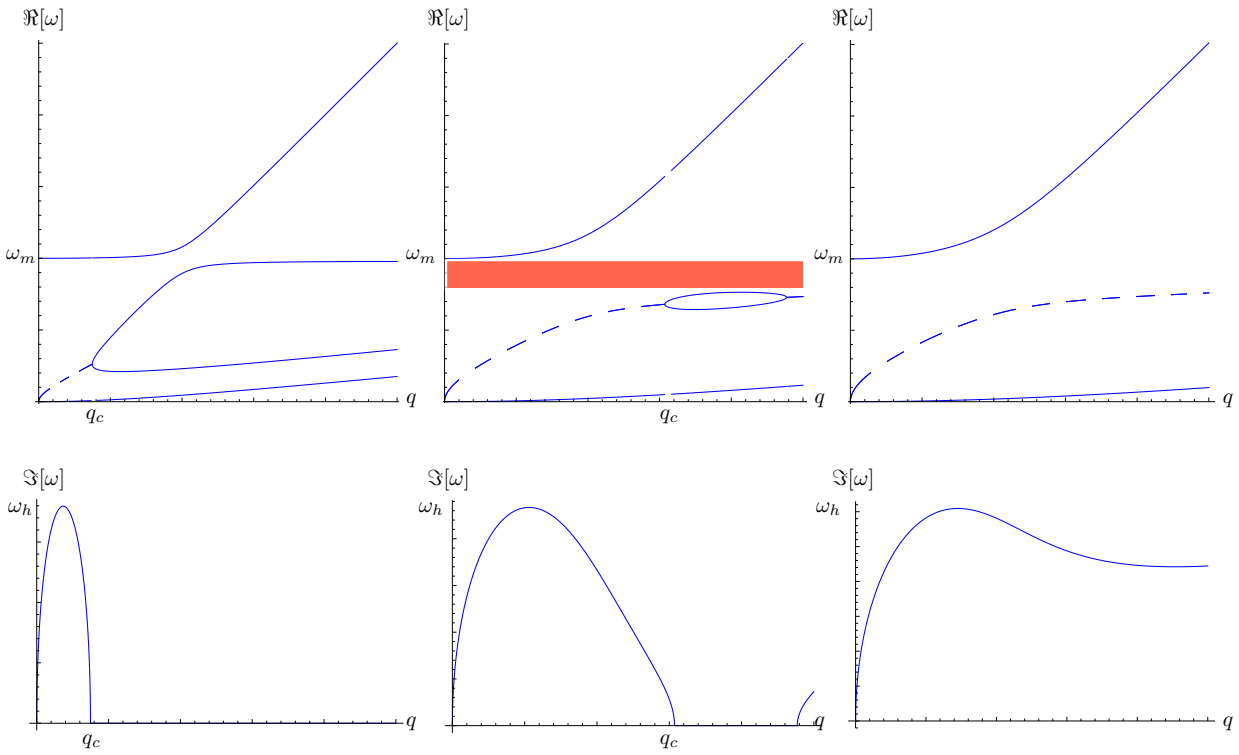

FIG. 1. The polariton spectra as we increase the magnetic field from left to right. Top: Real parts of the polariton poles, where the solid lines correspond to those with vanishing imaginary part while the dashed lines otherwise. Here, the magnon gap is given by $\omega_m = \gamma(Mm^2 + B_3)$ and the bifurcation starts at $q_c \approx 2egB_3/\left[\pi\gamma(Mm + \sqrt{MB_3})\right]$, which we estimate to be $\sim 10^{-5} - 10^{-4}$ A^{-1}. We have also shown the forbidden band for the intermediate value of magnetic field, depicted as the shaded region. Bottom: Imaginary part for the intermediate band, whose maximum value is given by ω_h, with $\omega_h \approx \sqrt{2}egB_3/\left[\pi\gamma(Mm + \sqrt{MB_3})\right]$.

on how much it overlaps with the single particle excitation regimes of the Weyl fermions. We find indeed that this overlap is negligible as the typical minimum energy needed to excite the Weyl fermions is about 10 meV (see Appx. A for details) while the typical magnon gap $\omega_m = \gamma(M\,m^2 + B_3)$ is about 0.1 meV[30].

Summary – In this article, we have shown that the topological response of magnons in Weyl semimetal is given by a non-local interaction between magnons and electromagnetic fields. This non-local interaction manifests itself in term of electric-field-induced magnetization dynamics that results in gapless magnon excitations. It also gives rise to resonant behavior in the form of magnon polariton featuring sibling bands and forbidden band.

Acknowledgements – We would like to thank Gerald Mahan, Xiaoliang Qi, Cenke Xu and Jainendra Jain for insightful discussions. J. H. is supported by NSF grant DMR-1005536 and DMR-0820404 (Penn State MRSEC). J. Z. is supported by the Theoretical Interdisciplinary Physics and Astrophysics Center and by the U.S. Department of Energy, Office of Basic Energy Sciences, Division of Materials Sciences and Engineering under Award DEFG02-08ER46544. R. R. is supported by the U.S. Department of Energy under contract DE-SC0008745.

Appendix A: 4-band model calculations

Let us start with the 4-band model of Ref. 12

$$H = H_0 + H_1, \tag{A1}$$

where

$$H_0 = \begin{pmatrix} \mathcal{M}+M & 0 & -i\,L_1\,k_3 & i\,L_2\,k_- \\ 0 & \mathcal{M}-M & -i\,L_2\,k_+ & -i\,L_1\,k_3 \\ i\,L_1\,k_3 & i\,L_2\,k_- & -\mathcal{M}+M & 0 \\ -i\,L_2\,k_+ & i\,L_1\,k_3 & 0 & -\mathcal{M}-M \end{pmatrix}, \tag{A2}$$

with

$$\mathcal{M} = M_0 + M_1\, k_3^2 + M_2\, k_\parallel^2, \tag{A3}$$

$$k_\pm = k_1 \pm i\, k_2; \tag{A4}$$

and

$$H_1 = \mathrm{diag}(\tilde{g}\mu_3, -\tilde{g}\mu_3, \tilde{g}\mu_3, -\tilde{g}\mu_3) = \tilde{g}\mu_3\sigma_3 \cdot \mathbb{1}_{2\times 2}. \tag{A5}$$

Here, we have magnetized the system along the $\hat{x}_3$-direction with magnetization M and for simplicity, allow magnetic fluctuations only along that same direction, where $\tilde{g} \ll 1$. All the material related parameters are defined in Ref. 12.

For $|M| > |M_0|$, this model exhibits Weyl points. Expanding around these Weyl points, one can obtain the low energy effective theory of Weyl fermions coupled chirally to the magnetic fluctuations as in Eq. (1). In particular, the axial vector field can then be related to the magnetic fluctuations as

$$a_3 = -\frac{M}{L_1\sqrt{M^2 - M_0^2}}\mu_3. \tag{A6}$$

For details, see Ref. 12.

Let us now turn on the external uniform magnetic field $\mathbf{B} = B\,\hat{x}_3$. The conjugate momenta on the direction perpendicular to the magnetic field become $k_+ \to \Pi_+ = \sqrt{2}\,a/\ell_c$ and $k_- \to \Pi_- = \sqrt{2}\,a^\dagger/\ell_c$, where a and $a^\dagger$ are the annihilation and creation operators for the Landau levels, respectively, and ℓ_c is the magnetic length. Since $a\,\phi_n = \sqrt{n}\,\phi_{n-1}$ and $a^\dagger\,\phi_n = \sqrt{n+1}\,\phi_{n+1}$, writing the wave function as

$$\phi = \begin{pmatrix} f_1^n\,\phi_{n-1} \\ f_2^n\,\phi_n \\ f_3^n\,\phi_{n-1} \\ f_4^n\,\phi_n \end{pmatrix}, \tag{A7}$$

the Hamiltonian then can be written as

$$H_{\mathrm{LL}} = \begin{pmatrix} \mathcal{M}_n + M & 0 & -i\,L_1\,k_3 & \frac{i\sqrt{2}L_2}{\ell_c}\sqrt{n} \\ 0 & \mathcal{M}_n - M & -\frac{i\sqrt{2}L_2}{\ell_c}\sqrt{n} & -i\,L_1\,k_3 \\ i\,L_1\,k_3 & \frac{i\sqrt{2}L_2}{\ell_c}\sqrt{n} & -\mathcal{M}_n + M & 0 \\ -\frac{i\sqrt{2}L_2}{\ell_c}\sqrt{n} & i\,L_1\,k_3 & 0 & -\mathcal{M}_n - M \end{pmatrix}, \tag{A8}$$

where

$$\mathcal{M}_n = M_0 + M_1\,k_3^2 + \frac{2M_2}{\ell_c^2}\left(n - \frac{1}{2}\right). \tag{A9}$$

Diagonalizing this Hamiltonian, we can then obtain the Landau levels for $n > 0$. For $n = 0$, this Hamiltonian is reduced to half in size

$$H_{\mathrm{LLL}} = \begin{pmatrix} \mathcal{M}_0 - M & -i\,L_1\,k_3 \\ i\,L_1\,k_3 & -\mathcal{M}_0 - M \end{pmatrix}. \tag{A10}$$

The resulting Landau levels are plotted in Fig. 2.

We can now perturb the above Hamiltonian by applying an external electric field $\mathbf{E} = E\,\hat{x}_3$ and ask what the response of the system to the axial vector field is. The response function is given by

$$\begin{aligned} \Pi_{aE}(\omega, q\hat{x}_3) &= \frac{\delta^2 S}{\delta a_3\,\delta E} \\ &= \frac{eB}{2\pi\ell_3}\sum_{n,n'\in LL}\sum_{k_3}\frac{n_F[\varepsilon_n(k_3)] - n_F\left[\varepsilon_{n'}(k_3+q)\right]}{\omega + \varepsilon_n(k_3) - \varepsilon_{n'}(k_3+q)}\,(i\,\tilde{g}\,e)\,\langle n', k_3+q|\mathbb{I}_{4\times 4}|n, k_3\rangle \\ &\qquad \left(-\frac{L_1\sqrt{M^2 - M_0^2}}{M}\right)\langle n, k_3\,|\sigma_3\cdot\mathbb{I}_{2\times 2}|\,n', k_3+q\rangle. \end{aligned} \tag{A11}$$

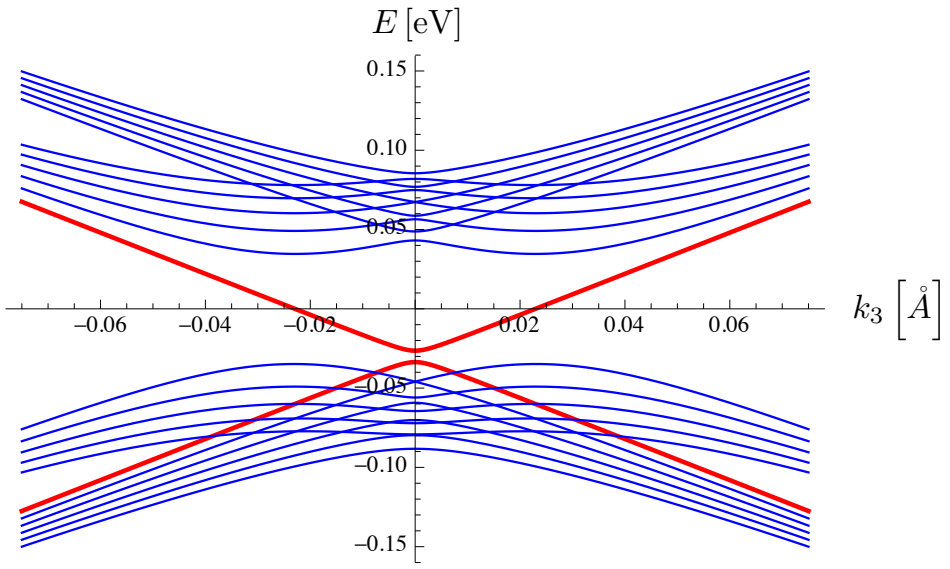

FIG. 2. Landau levels for $M_0 = -0.005$ eV, $M_1 = 0.342$ eV·Å^2, $M_2 = 18.225$ eV·Å^2, $L_1 = 1.3$ eV·Å, $L_2 = 2.82$ eV·Å^2 and $B = 5$T. $n = 0$ Landau levels are depicted in red, while the higher Landau levels are depicted in blue.

Here, n_F is Fermi distribution, ℓ_3 is the length of the system in $\hat{x}_3$ direction and the factor $e\,B$ comes from the degeneracy of Landau levels. We can approximate this by neglecting the contribution from higher Landau levels

$$\Pi_{aE}(\omega, q\,\hat{x}_3) = \frac{L_1\sqrt{M^2 - M_0^2}}{M}\,\frac{i\,\tilde{g}\,e^2\,B}{2\pi\ell_3}\sum_{n,n'\in \mathrm{LLL}}\sum_{k_3}\frac{n_F[\varepsilon_n(k_3)] - n_F\left[\varepsilon_{n'}(k_3+q)\right]}{\omega + \varepsilon_n(k_3) - \varepsilon_{n'}(k_3+q)}\left|\langle n', k_3+q|n, k_3\rangle\right|^2, \tag{A12}$$

where we have projected the matrix elements of the interaction Hamiltonian H_1 (which is 4×4) into the LLL space (which is 2×2). For $T = 0$, $\mu = 0$ and small q, we therefore have

$$\begin{aligned}\Pi_{aE}(\omega \ll q, q\,\hat{x}_3) &\approx \left[L_1^4 + 4L_1^2M_0M_1 + 4M_1^2M^2 - (2M_0M_1 + L_1^2)\sqrt{L_1^4 + 4L_1^2M_0M_1 + 4M_1^2M^2}\right]^{-\frac{1}{2}} \\ &\quad \sqrt{2}\,\pi\,|M_1|\,L_1\sqrt{M^2 - M_0^2}\,\frac{\tilde{g}\,e^2\,B}{\pi^2\,(-i\,q)} \\ &\equiv \frac{g\,e^2\,B}{\pi^2}\left(\frac{-i\,q}{-q^2}\right).\end{aligned} \tag{A13}$$

The Lagrangian density in momentum space is then given by

$$\mathcal{L} = \Pi_{aE}\,E\,a_3 = \frac{g\,e^2}{\pi^2}\,E\,B\left(\frac{-i\,q}{-q^2}\right)a_3, \tag{A14}$$

which upon Fourier transforming back to real space, reads

$$\mathcal{L} = -\frac{g\,e^2}{\pi^2}\,E(x)\,B(x)\,\nabla_y G(x-y)\cdot\mathbf{a}(y), \tag{A15}$$

in agreement with Eq. (4).

Next, let us look at the polarization operator in the presence of the external magnetic field. The regime where its imaginary part is non-vanishing corresponds to the regime of single particle excitations (SPE) of the Weyl fermions. Since we are interested in comparing it to the spectrum of the polariton, we are going to focus on the case where the momentum is perpendicular to the direction of the magnetic field $\mathbf{q} = \mathbf{q}_\parallel$. The polarization operator is then given by

$$\begin{aligned}\Pi_{EE}(\omega, \mathbf{q}_\parallel) &= \frac{\delta^2 S}{(\delta E)^2} \\ &= \frac{e^3\,B}{2\pi\ell_3}\sum_{n,n'}\sum_{k_3}\frac{n_F[\varepsilon_n(k_3)] - n_F\left[\varepsilon_{n'}(k_3)\right]}{\omega + \varepsilon_n(k_3) - \varepsilon_{n'}(k_3) + i0^+}\left|\langle n', k_3|n, k_3\rangle\right|^2.\end{aligned} \tag{A16}$$

We note that the right hand side does not depend on $\mathbf{q}_\parallel$. Furthermore, the bottom boundary of the SPE regime is the smallest gap between the filled part of the lowest Landau level and the second Landau level. As can be seen from Fig. 2, it is of order 0.03 eV.

Appendix B: The Constant Vector Limit

Let us start by putting our theory, Eq. (4), in a finite volume by introducing a finite volume regulator $a^\mu(y) \to a^\mu(y) \exp\left[-|\hat{a}\cdot y|/\Lambda\right]$, such that

$$S_{\rm top} = -\frac{e^2 g}{8\pi^2}\int d^4x\, d^4y\, \varepsilon^{\alpha\beta\gamma\delta}\, F_{\alpha\beta}(x)\, F_{\gamma\delta}(x)\, \frac{\partial G(x-y)}{\partial y^\mu}\, a^\mu(y) e^{-\frac{|\hat{a}\cdot y|}{\Lambda}}, \tag{B1}$$

where $\Lambda \gg L$ and L is the typical size of the system. We note that when the axial vector field goes to a constant vector limit, the field strength $\partial_\mu\left[a_\nu(y)\exp\left(-|\hat{a}\cdot y|/\Lambda\right)\right] - \partial_\nu\left[a_\mu(y)\exp\left(-|\hat{a}\cdot y|/\Lambda\right)\right]$, which includes the curl $\nabla \times [\mathbf{a}\,\exp(-|\hat{a}\cdot y|/\Lambda)]$, remains vanishing while the divergence $\partial_\mu[a^\mu\,\exp(-|\hat{a}\cdot y|/\Lambda)]$ remains non-zero. Therefore, even at the constant vector limit, the magnon is Helmholtz decomposed into the curl-free term only.

In order to obtain the constant vector limit of Eq. (B1), we write $a^\mu \exp(-|\hat{a}\cdot y|/\Lambda) = g^{\mu\nu}\,\partial_\nu\left[a\cdot y\,\exp(-|\hat{a}\cdot y|/\Lambda)\right] + \mathcal{O}(1/\Lambda)$. Substituting it in Eq. (4) and integrating by parts, we obtain

$$\begin{aligned} S_{\rm top} = &-\frac{e^2 g}{8\pi^2}\int d^4x\, d^4y\, \varepsilon^{\alpha\beta\gamma\delta}\, F_{\alpha\beta}(x)\, F_{\gamma\delta}(x)\, \partial_\nu\left[g^{\mu\nu}\frac{\partial G(x-y)}{\partial y^\mu}\, a\cdot y\, e^{-\frac{|\hat{a}\cdot y|}{\Lambda}}\right] \\ &+\frac{e^2 g}{8\pi^2}\int d^4x\, d^4y\, \varepsilon^{\alpha\beta\gamma\delta}\, F_{\alpha\beta}(x)\, F_{\gamma\delta}(x)\, \Box_y G(x-y)\, a\cdot y\, e^{-\frac{|\hat{a}\cdot y|}{\Lambda}}. \end{aligned} \tag{B2}$$

The first term is the surface term that vanishes due to the regulator and using the definition of the Green's function we recover the action in the Ref. 23

$$S_{\rm top} \to \frac{e^2 g}{8\pi^2}\int d^4x\, \varepsilon^{\alpha\beta\gamma\delta}\, F_{\alpha\beta}(x)\, F_{\gamma\delta}(x)\, (a\cdot x). \tag{B3}$$

Appendix C: The Polariton Green Function

Setting $\mathbf{B} = B\hat{x}_3$ and then applying an electric field along the $\hat{x}_3$ direction, the Landau-Lifshitz and Maxwell equations can be written as

$$\mathcal{E}(\omega, q)\begin{pmatrix} \frac{\mathbf{q}_\parallel\cdot\mathbf{a}_\parallel}{q} \\ E_3 \end{pmatrix} = 0, \tag{C1}$$

where $|\mathbf{q}_\parallel| = q$ and

$$\mathcal{E}(\omega,q) = \begin{pmatrix} \frac{\omega^2}{\gamma^2 M^2} - \left(J\,q^2 + m^2 + \frac{B_3}{M}\right)^2 & \frac{e^2 g}{\pi^2}\frac{iq(J\,q^2+m^2+B_3/M)B_3}{\omega^2 - v_F^2\,q^2} \\ -\frac{e^2 g}{\pi^2}\frac{i\,q\,\omega^2\,B_3}{\omega^2 - v_F^2\,q^2} & \omega^2 - q^2 \end{pmatrix}. \tag{C2}$$

The Green function for the polariton then must satisfy

$$\mathcal{E}(\omega,q)\,\mathcal{G}(\omega,q) = \mathbb{I}_{2\times 2}, \tag{C3}$$

and its singularities are given by the singularities of $\mathcal{E}^{-1}$, which are the zeroes of $\det\mathcal{E}$. We note that the solutions to $\det\mathcal{E} = 0$ are identical to the solutions of Eq. (13). Furthermore, we can obtain the spectral density from $\rho(\omega,q) = \Im[\mathcal{G}(\omega,q)]$. The spectral densities of the top and bottom band are trivial as they correspond to well-defined quasiparticles, while the spectral density of the intermediate band exhibits finite width. In Fig. 3, we plot the spectral density of the intermediate band at small magnetic field for different values of momenta up to $q = 0.99 q_c$, where q_c is the momentum at which bifurcation into the "sibling" bands occur.

* jah77@psu.edu

[1] N. Nielsen, H. Romer, and B. Schroer, Phys. Lett. B **70**,

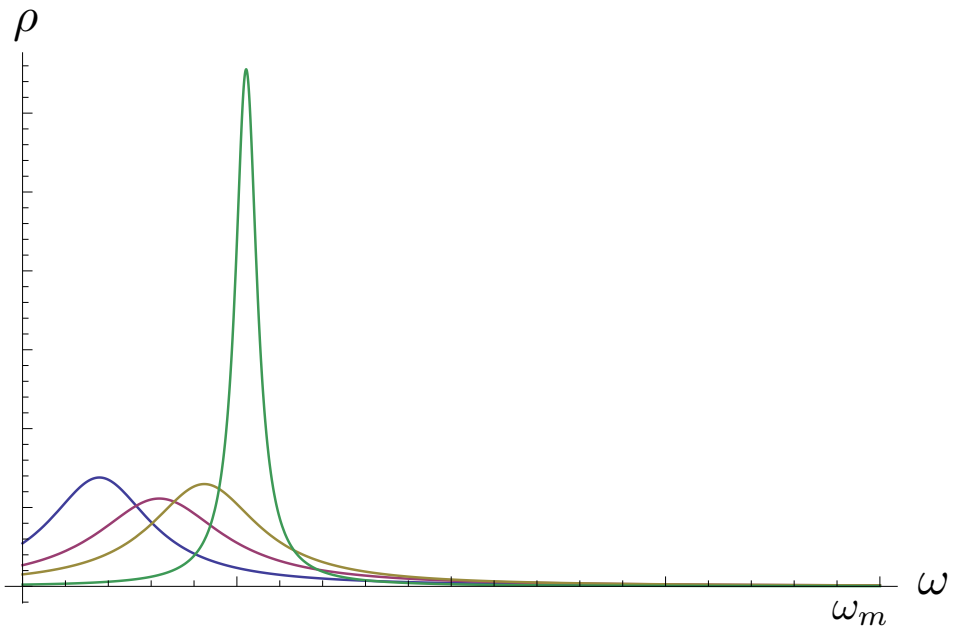

FIG. 3. The spectral density at small magnetic field for different values of momenta $q/q_c = 0.2$, 0.5, 0.75 and 0.99 for the blue, purple, yellow and green lines (from left to right), respectively. Here, $q_c \approx 2egB_3/\left[\pi\gamma(Mm+\sqrt{MB_3})\right]$ is the momentum at which the bifurcation into the "sibling" bands starts and $\omega_m = \gamma(Mm^2 + B_3)$ is the magnon gap.

445 (1977).
[2] N. Nielsen, H. Romer, and B. Schroer, Nucl. Phys. B **136**, 475 (1978).
[3] L. Alvarez-Gaume and P. Ginsparg, Nucl. Phys. B **243**, 449 (1984).
[4] L. Alvarez-Gaume and P. Ginsparg, Annals of Physics **161**, 423 (1985).
[5] S. Ryu, J. E. Moore, and A. W. W. Ludwig, Phys. Rev. B **85**, 045104 (2012).
[6] Z. Wang, X.-L. Qi, and S.-C. Zhang, Phys. Rev. B **84**, 014527 (2011).
[7] M. Stone, Phys. Rev. B **85**, 184503 (2012).
[8] Z. Ringel and A. Stern, Phys. Rev. B **88**, 115307 (2013).
[9] P. Hosur and X. Qi, Comptes Rendus Physique (2013).
[10] A. Burkov and L. Balents, Phys. Rev. Lett. **107**, 127205 (2011), 1105.5138.
[11] G. Y. Cho, arXiv preprint arXiv:1110.1939 (2011).
[12] C.-X. Liu, P. Ye, and X.-L. Qi, Phys. Rev. B **87**, 235306 (2013), 1204.6551.
[13] C.-Z. Chang, J. Zhang, M. Liu, Z. Zhang, X. Feng, K. Li, L.-L. Wang, X. Chen, X. Dai, Z. Fang, X.-L. Qi, S.-C. Zhang, Y. Wang, K. He, X.-C. Ma, and Q.-K. Xue, Advanced Materials **25**, 1065 (2013).
[14] M. Srednicki, Quantum Field Theory (Cambridge University Press, 2007).
[15] When $f_{\mu\nu} = 0$, the solution to Dirac equation is given by $\psi = 0$. In this letter, we would like to obtain the effective interaction between magnons and electromagnetic fields by integrating out Weyl fermion fluctuations around the vacuum solution $\psi = 0$. However, when the flux of the axial vector field strength takes non-zero integer values, the solution to Dirac equation consists of additional $(1+1)$-dimensional Weyl fermions[12]. The topological response obtained by integrating out fermionic fluctuations around this non-trivial background will be studied elsewhere.
[16] X.-L. Qi, T. L. Hughes, and S.-C. Zhang, Phys. Rev. B **78**, 195424 (2008).
[17] S. L. Adler, Phys. Rev. **177**, 2426 (1969).
[18] J. S. Bell and R. Jackiw, Il Nuovo Cimento A **60**, 47 (1969).
[19] G. t Hooft and M. Veltman, Nuclear Physics B **44**, 189 (1972).
[20] S. Gottlieb and J. T. Donohue, Phys. Rev. D **20**, 3378 (1979).
[21] J. Hořejší, Czech. J. Phys. **42**, 345 (1992).
[22] J. A. Harvey, hep-th/0509097.
[23] A. A. Zyuzin and A. A. Burkov, Phys. Rev. B **86**, 115133 (2012).
[24] Z. Wang and S.-C. Zhang, Phys. Rev. B **87**, 161107 (2013).
[25] K.-Y. Yang, Y.-M. Lu, and Y. Ran, Phys. Rev. B **84**, 075129 (2011).
[26] Y. Chen, S. Wu, and A. A. Burkov, Phys. Rev. B **88**, 125105 (2013).
[27] G. D. Mahan, Many-Particle Physics, 3rd ed. (Springer, 2000).
[28] G. D. Mahan, Condensed matter in a nutshell (Princeton University Press, 2010).
[29] R. Li, J. Wang, X.-L. Qi, and S.-C. Zhang, Nature Physics **6**, 284 (2010).
[30] E. Popova, N. Keller, F. Gendron, M. Guyot, M.-C. Brianso, Y. Dumond, and M. Tessier, Journal of Applied Physics **90**, 1422 (2001).